arXiv:1409.2929v2 [quant-ph] 26 Aug 2015

T-shaped Single-photon Router

Jing Lu[1], Z. H. Wang[2] and Lan Zhou[1,*]

[1]*Synergetic Innovation Center of Quantum Effects and Applications, Department of Physics, Hunan Normal University, Changsha 410081, China*
[2] *Beijing Computational Science Research Center, Beijing 100084, China*

[*]*zhoulan@hunnu.edu.cn*

Abstract: We study the transport properties of a single photon scattered by a two-level system (TLS) in a T-shaped waveguide, which is made of two coupled-resonator waveguides (CRWs)— an infinite CRW and a semi-infinite CRW. The spontaneous emission of the TLS directs single photons from one CRW to the other. Although the transfer rate is different for the wave incident from different CRWs, due to the boundary breaking the translational symmetry, the boundary can enhance the transfer rate found in Phys. Rev. Lett. 111, 103604 (2013) and Phys. Rev. A 89, 013805 (2014), as the transfer rate could be unity for the wave incident from the semi-infinite CRW.

© 2015 Optical Society of America

OCIS codes: (270.0270) Quantum optics; (230.4555) Coupled resonators; (270.5585) Quantum information and processing.

References and links

1. H.J. Kimble, "The quantum internet," Nature (London) **453**, 1023-1030 (2008).
2. J.T. Shen and S. Fan, "Coherent single photon transport in a one-dimensional waveguide coupled with superconducting quantum bits," Phys. Rev. Lett. **95**, 213001 (2005).
3. J.T. Shen and S. Fan, "Theory of single-photon transport in a single-mode waveguide. I. coupling to a cavity containing a two-level atom," Phys. Rev. A **79**, 023837 (2009).
4. J.T. Shen and S. Fan, "Theory of single-photon transport in a single-mode waveguide. II. coupling to a whisperinggallery resonator containing a two-level atom," Phys. Rev. A **79**, 023838 (2009).
5. L. Zhou, Z.R. Gong, Y.-x. Liu, C.P. Sun, and F. Nori, "Controllable scattering of a single photon inside a one-dimensional resonator waveguide," Phys. Rev. Lett. **101**, 100501 (2008).
6. L. Zhou, S. Yang, Yu-xi Liu, C.P. Sun and F. Nori, "Quantum zeno switch for single-photon coherent transport," Phys. Rev. A **80**, 062109 (2009).
7. Q. Li, L. Zhou, and C.P. Sun, "Waveguide quantum electrodynamics: controllable channel from quantum interference," Phys. Rev. A **89**, 063810 (2014).
8. L. Zhou, H. Dong, Y.-x. Liu, C.P. Sun, and F. Nori, "Quantum supercavity with atomic mirrors," Phys. Rev. A **78**, 063827 (2008).
9. Z.R. Gong, H. Ian, L. Zhou, and C.P. Sun, "Controlling quasibound states in a one-dimensional continuum through an electromagnetically-induced-transparency mechanism," Phys. Rev. A **78**, 053806 (2008).
10. H. Dong, Z.R. Gong, H. Ian, L. Zhou and C.P. Sun, "Intrinsic cavity QED and emergent quasinormal modes for a single photon," Phys. Rev. A **79**, 063847 (2009).
11. J.Q. Liao, Z.R. Gong, L. Zhou, Y.X. Liu, C.P. Sun and F. Nori, "Controlling the transport of single photons by tuning the frequency of either one or two cavities in an array of coupled cavities," Phys. Rev. A **81**, 042304 (2010).
12. T.S. Tsoi and C. K. Law, "Quantum interference effects of a single photon interacting with an atomic chain inside a one-dimensional waveguide," Phys. Rev. A **78**, 063832 (2008).
13. T.S. Tsoi and C. K. Law, "Single-photon scattering on Λ-type three-level atoms in a one-dimensional waveguide," Phys. Rev. A **80**, 033823 (2009).
14. D Witthaut and A.S. Sørensen, "Photon scattering by a three-level emitter in a one-dimensional waveguide," New J. Phys. **12**, 043052 (2010).

15. C.-H. Yan, L.-F. Wei, W.-Z. Jia, and J.-T. Shen, "Controlling resonant photonic transport along optical waveguides by two-level atoms," Phys. Rev. A **84**, 045801 (2011).
16. Y.-C. Shen, M. Bradford, and J.-T. Shen, "Single-photon diode by exploiting the photon polarization in a waveguide," Phys. Rev. Lett. **107**, 173902 (2011).
17. L. Zhou, Y. Chang, H. Dong, L.M. Kuang, and C.P. Sun, "Inherent Mach-Zehnder interference with which-way detection for single-particle scattering in one dimension," Phys. Rev. A **85**, 013806 (2012).
18. M. Bradford, K.C. Obi, and J.-T. Shen, "Efficient single-photon frequency conversion using a sagnac interferometer," Phys. Rev. Lett. **108**, 103902 (2012).
19. Z.H. Wang, L. Zhou, Y. Li, and C. P. Sun, "Controllable single-photon frequency converter via a one-dimensional waveguide," Phys. Rev. A **89**, 053813 (2014).
20. L. Zhou, L.P. Yang, Y. Li, and C.P. Sun, "Quantum routing of single photons with a cyclic three-level system," Phys. Rev. Lett. **111**, 103604 (2013).
21. J. Lu, L. Zhou, L.M. Kuang, and F. Nori, "Single-photon router: Coherent control of multichannel scattering for single photons with quantum interferences," Phys. Rev. A **89**, 013805 (2014).
22. J.P. Albert, C. Jouanin, D. Cassagne, and D. Bertho, "Generalized Wannier function method for photonic crystals," Phys. Rev. B **61**, 4381-4384 (2000).
23. N. Malkova and V. Gopalan, "Strain-tunable optical valves at T-junction waveguides in photonic crystals," Phys. Rev. B **68**, 245115 (2003).
24. T. Herrle, S. Schmult, M. Pindl, U.T. Schwarz, and W. Wegscheider, "T-shaped waveguides for quantum-wire intersubband lasers," Phys. Rev. B **72**, 035316 (2005).
25. E. Bulgakov and A. Sadreev, "Symmetry breaking in a T-shaped photonic waveguide coupled with two identical nonlinear cavities," Phys. Rev. B **84**, 155304 (2011).
26. I. Buluta, S. Ashhab and F. Nori, "Natural and artificial atoms for quantum computation," Reports on Progress in Physics **74** 104401 (2011).
27. I. Buluta, F. Nori, " Quantum simulators," Science **326**, 108-111 (2009).
28. I. M. Georgescu, S. Ashhab and F. Nori, " Quantum simulators," Rev. Mod. Phys. **86**, 153-185 (2014).
29. J.Q. You and F. Nori " Superconducting circuits and quantum information," Physics Today **58** (11), 42-47 (2005).
30. J.Q. You and F. Nori " Atomic physics and quantum optics using superconducting circuits," Nature **474**, 589-597 (2011).
31. Z.L. Xiang, S. Ashhab, J.Q. You and F. Nori "Hybrid quantum circuits: superconducting circuits interacting with other quantum systems," Rev. Mod. Phys. **85**, 623-653 (2013).
32. K.G. Makris and D.N. Christodoulides, "Method of images in optical discrete systems," Phys. Rev. E **73**, 036616 (2006).

1. Introduction

Quantum channels and nodes are the building blocks of quantum networks [1]. Photons are natural carriers in quantum channels due to their robustness in preserving quantum information during propagation. Quantum channels are made of waveguides, which means that controlling photons coherently in a confined geometry is of both fundamental and practical importance for building quantum networks. Due to the negligible interaction among individual photons, quantum devices at single-photon level have been proposed based on the interaction of confined propagating fields with single atoms [2–19]. As a quantum network has more than one quantum channel, a multichannel quantum router [20,21] for single photons has been explored to transfer single photons from one quantum channel to the other.

There are two ways to change the transport properties of particles in quantum channels: the incorporation of impurities, or slight structural variations. Quantum routers in [20, 21] have made good use of the arrangement of the energy configuration of single atoms. In this paper, we propose a single-photon routing scheme using a two-level system (TLS). Different from the studies in [20, 21], where two infinite one-dimensional (1D) coupled-resonator waveguides (CRWs) form a X-shaped waveguide, we consider a slight structural variation of the two 1D CRWs, i.e., one 1D CRW is infinite and the other is semi-infinite, which form a T-shaped waveguide [22–25]. The systems studies here, could be implemented using, e.g., artificial atoms [26–28] coupled to superconducting circuits [29–31]. Aiming to answer the question whether the boundary can enhance the transfer rate found in [20, 21], we studied the single-photon scattering process by the TLS, and found that: the spontaneous emission of the

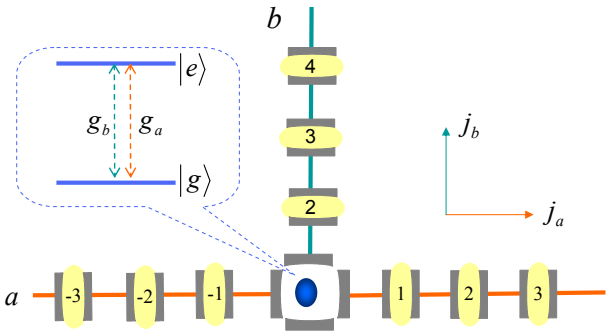

Fig. 1. Schematic view of quantum routing of single photons in two channels made of one infinite and one semi-infinite CRWs. The two-level atom characterized by $|g\rangle$, $|e\rangle$ is placed at the cross point $j_a = 0$ and $j_b = 1$. CRW-a (-b) couples to the atom through the transition $|g\rangle \leftrightarrow |e\rangle$ with strength g_a (g_b). There is no interaction among the $j_a = 0$ and $j_b = 1$ cavities

TLS routes single photon from one CRW to the other; the probability for finding single photon in one CRW is different for waves incident from different CRWs, due to the boundary breaking the translational symmetry; The probability for finding single photon in the infinite CRW could reach one for waves incident from the semi-infinite CRW, however, 50% is the maximum transfer rate in [20, 21].

This paper is organized as follows: In Sec. 2, the T-shaped waveguide with a TLS embedded in its junction is introduced. In Sec. 3, the single-photon scattering process is studied for waves incident from different CRWs. Finally, we conclude with a brief summary of the results.

2. Model setup

A 1D CRW is made of single-mode cavities which are coupled to each other through the evanescent tails of adjacent fields resulting in photon hopping among neighbouring cavities. Here, we consider two 1D CRWs which form a T-shaped waveguide. As sketched in Fig. 1, coupled resonators on the red (green) line construct the infinite (semi-infinite) CRW, which is called CRW-a (CRW-b) hereafter. We note that we have introduced a boundary in one of the CRWs in [20, 21]. The purpose of classifying cavities in Fig. 1 into the CRW-a and -b is for the convenience to compare the results with those in [20, 21]. The cavity modes of the two 1D CRWs are described by the annihilation operators a_{j_a} and b_{j_b}, respectively. Here, subscripts $j_a = -\infty, \cdots, +\infty$ and $j_b = 1, \cdots, +\infty$. The Hamiltonian of each CRW is described by a typical tight-binding bosonic model. The free propagation of the photons in the T-shaped waveguide is described by

$$H_C = \sum_{d=a,b} \sum_{j_d} \left[\omega_d d_{j_d}^\dagger d_{j_d} - \xi_d \left(d_{j_d}^\dagger d_{j_d+1} + \text{h.c.} \right) \right], \tag{1}$$

where we have assumed that all cavities in the CRW a (b) have the same frequency ω_a (ω_b) and the hopping energies ξ_a (ξ_b) between any two nearest-neighbor cavities in the CRW-a (b) are the same. We note that there is no interaction between the $j_a = 0$ and $j_b = 1$ cavities.

A TLS (an atom, a quantum dot, or a superconducting qubit) described by the free Hamiltonian

$$H_A = \omega_A |e\rangle \langle e| \tag{2}$$

is placed at the node of the T junction, where ω_A is its energy splitting. The TLS characterized by a ground state $|g\rangle$ and an excited state $|e\rangle$ is coupled at a rate g_a (g_b) to the cavity at $j_a = 0$

($j_b = 1$). The interaction between the TLS and quantized electromagnetic modes reads

$$H_{AC} = g_a \sigma_+ a_0 + g_b \sigma_+ b_1 + h.c. \tag{3}$$

where the operators $\sigma_\pm$ are the ladder operators of the TLS. The dynamics of the total system is governed by Hamiltonian $H = H_C + H_A + H_{AC}$.

The Hamiltonian (1) can be exactly diagonalized as $H_C = \sum_{d=a,b} E_{k_d} d_{k_d}^\dagger d_{k_d}$ by the Fourier transformations $a_{k_a} = \frac{1}{\sqrt{2\pi}} \int d j_a a_{j_a} e^{i k_a j_a}$ and $b_{k_b} = \sqrt{\frac{2}{\pi}} \int d j_b b_{j_b} \sin(k_b j_b)$ for the CRW-a and -b respectively. The dispersion relation of both CRWs

$$E_{k_d} = \omega_d - 2\xi_d \cos k_d \tag{4}$$

is a cosine function of the wavenumber k_d ($d = a, b$), which indicates that each CRW possesses an energy band with bandwidth $4\xi_d$. Consequently, two quantum channels (i.e., two broad continua of propagating modes) are formed.

3. Single-photon quantum router

Since the operator $N = \sum_{d=a,b} \sum_{j_d} d_{j_d}^\dagger d_{j_d} + \sigma_+ \sigma_-$ commutes with Hamiltonian H, the total number of excitations is a conserved quantity. To find the scattering equation in the single-excitation subspace, the eigenstate of the full Hamiltonian is assumed to be

$$|E\rangle = \sum_{d=a,b} \sum_{j_d=-\infty}^{+\infty} U_{j_d}^{[d]} d_{j_d}^\dagger |g0\rangle + U_e |e0\rangle, \tag{5}$$

where $|0\rangle$ is the vacuum state of the T-shaped waveguide, $U_{j_a}^{[a]}$ ($U_{j_b}^{[b]}$) is the probability amplitudes of the photon in the j_ath (j_bth) cavity of the CRW-a (CRW-b), and U_e is the atomic excitation amplitude. The eigenequation gives rise to a series of coupled stationary equations for all amplitudes

$$\begin{aligned}
E U_j^{[a]} &= \omega_a U_j^{[a]} - \xi_a \left(U_{j-1}^{[a]} + U_{j+1}^{[a]} \right) + g_a U_e \delta_{j0} && (6)\\
E U_j^{[b]} &= \omega_b U_j^{[b]} - \xi_b \left(U_{j-1}^{[b]} + U_{j+1}^{[b]} \right) + \delta_{j1} g_b U_e && (7)\\
E U_e &= \omega_A U_e + g_a U_0^{[a]} + g_b U_d^{[b]} && (8)
\end{aligned}$$

where $\delta_{mn} = 1\ (0)$ for $m = n$ ($m \neq n$). Removing the atomic amplitude leads to the scattering equations for single photons

$$\begin{aligned}
(E - \omega_a) U_j^{[a]} &= -\xi_a \left(U_{j-1}^{[a]} + U_{j+1}^{[a]} \right) + \delta_{j0} \left[V_a(E) U_0^{[a]} + G(E) U_1^{[b]} \right] && (9)\\
(E - \omega_b) U_1^{[b]} &= -\xi_b U_2^{[b]} + G(E) U_0^{[a]} + V_b(E) U_1^{[b]} && (10)\\
(E - \omega_b) U_j^{[b]} &= -\xi_b \left(U_{j-1}^{[b]} + U_{j+1}^{[b]} \right) (j \geq 2). && (11)
\end{aligned}$$

The coupling between the TLS and CRWs gives rise to the energy-dependent deltalike potentials with strength $V_d(E) = g_d^2/(E - \omega_A)$ and the effective dispersive coupling strength $G(E) = g_a g_b/(E - \omega_A)$ between two CRWs, which are highly localized.

In this paper, we are interested in routing single photons from one CRW to the other, i.e., the TLS acts as a multichannel quantum router. According to the results in [20, 21], we set $\omega_a = \omega_b = \omega$ and $\xi_a = \xi_b = \xi$ in the following discussion. Since the boundary of the CRW-b breaks the translational symmetry, we solve Eqs.(9-11) for waves incoming from both CRWs separately.

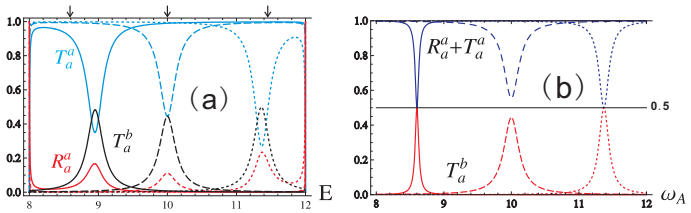

Fig. 2. The probability for finding single photons. (a) The transmission $T_a^a(E)$ (blue line), reflection R_a^a (red line) $T_a^b(E)$ (black line) as a function of the incident energy E, where the parameters are set as follow: $\omega_A = 9$ for solid line, $\omega_A = 10$ for dashed line, $\omega_A = 11.3$ for dotted line, and the coupling strength $g_a = g_b = 0.3$, (b) The coefficient $R_a^a(E) + T_a^a(E)$ (blue line), $T_a^b(E)$ (red line) as a function of the atomic energy splitting ω_A, where the parameters are set as follow: $g_a = g_b = 0.15, E = 10 - \sqrt{2}$ for solid line, $g_a = g_b = 0.3, E = 10$ for dotted line, $g_a = g_b = 0.25, E = 10 + \sqrt{2}$ for dashed line. All the parameters are in units of ξ, and we always set $\omega = 10$. The arrows in (a) indicate the position of the incident energy E of the solid, dashed and dotted lines in (b).

3.1. Single photons incident from the infinite CRW-a

For a photon with wavenumber k incident along the j_a axis onto the T-shaped waveguide, it will be absorbed by the TLS, which transits from its ground state to its excited state. Since the excited state is coupled to the continua of states, the excited TLS will emit a photon spontaneously into the propagating state of either CRW-a or CRW-b. Then a scattering process of single photons is completed, i.e., waves encoutering the TLS result in reflected, transmitted, and transferred waves with the same energy $E = \omega - 2\xi\cos k$. The boundary forces the photon within a certain region of space. We search for a solution of Eqs.(9)-(11) in the form

$$U_{j_a}^{[a]} = \begin{cases} e^{ikj_a} + re^{-ikj_a}, & j_a < 0 \\ te^{ikj_a}, & j_a > 0 \end{cases} \tag{12}$$

$$U_{j_b}^{[b]} = \begin{cases} t^b e^{ikj_b}, & j_b > 1 \\ A\sin kj_b, & j_b = 1 \end{cases} \tag{13}$$

where r, t, and t^b are the reflection, transmission, and transfer amplitudes respectively, and A is the amplitude at the boundary cavity $j_b = 1$. Substitution of Eqs.(12)-(13) into Eqs.(9)-(11), after some algebra, we obtain the relation $U_0^{[a]} = t = 1 + r$, and

$$t = \frac{v_g(E-\omega_A) + \sin(2k)g_b^2 + i2g_b^2\sin^2 k}{v_g(E-\omega_A) + g_b^2\sin(2k) + i\left(g_a^2 + 2g_b^2\sin^2 k\right)}, \tag{14}$$

$$t^b = \frac{-2g_a g_b \sin k}{v_g(E-\omega_A) + g_b^2\sin(2k) + i\left(g_a^2 + 2g_b^2\sin^2 k\right)}, \tag{15}$$

where the group velocity $v_g = 2\xi\sin k$. It can be verified that the scattering amplitudes satisfy $|t|^2 + |r|^2 + \left|t^b\right|^2 = 1$, which indicates probability conservation for the photon. It can be found in Eqs. (14)-(15) that when $g_b = 0$, $t^b = 0$, and the transmission amplitude t is the same as the one obtained in [5], where the system showed the resonant scattering at energy $E = \omega_A$ and $\Gamma_a(E) = g_a^2/v_g$ is regarded as the width of the resonance, or the decay rate of the TLS into the modes of the CRW-a. However, there is no frequency shift of the atom. It can be found in Eq.(15) that the coupling between the waveguide and the TLS that plays the important role on transferring single photon from one quantum channel to the other.

In Fig. 2, we plot transmission $T_a^a(E) = |t|^2$ (blue line), reflection $R_a^a = |r|^2$ (red line), $T_a^b(E) = \left|t^b\right|^2$ (black line) as well as coefficients $T_a^a + R_a^a$ (blue line) and T_a^b (red line) as a

function of the incident energy E. We note that $T_a^a + R_a^a$ (T_a^b) gives the probability for finding a single photon in the CRW-$a(b)$. It can be observed that: 1) the maximum transfer rate is 50%; 2) Although the magnitudes of the probabilities are dependent on the atomic energy splitting, the energy splitting of the TLS is no longer the position of the peak; 3) The product of the coupling strengths determines the width of the lineshape. Comparing to the observations in [20, 21], the only difference is the resonant-scattering energy, i.e., the second observation here.

3.2. Single photons incident from the semi-infinite CRW-b

Now, we consider that a plane Bloch wave of a single photon is launched from the upper to the bottom along the $-j_b$ axis into the semi-infinite CRW-b with the dispersion relation $E = \omega - 2\xi\cos k$. When the traveling photon arrives at the node of the T junction, it is either absorbed by the TLS or reflected by the boundary. The fraction reflected by the boundary propagates along the positive j_b axis. The portion absorbed by the TLS is reemitted into the waveguide. The emitted radiation propagates into two directions in the CRW-a, namely the forward and backward directions along the CRW-a. In the CRW-b, the TLS radiates the photon to the upwards and downwards, the photon originally radiated to the downwards is retroreflected to the TLS, since the termination of the CRW-b imposes a hard-wall boundary condition on the field which behaves as a perfect mirror. The probability amplitudes in the asymptotic regions are given by

$$U_{j_a}^{[a]} = \begin{cases} t_l^a e^{-ikj_a}, & j_a < 0 \\ t_r^a e^{ikj_a}, & j_a > 0 \end{cases} \tag{16}$$

$$U_1^{[b]} = A\sin k, \quad j_b = 1 \tag{17}$$

$$U_{j_b}^{[b]} = e^{-ikj_b} + r^b e^{ikj_b}, \quad j_b > 1, \tag{18}$$

where t_r^a (t_l^a) and r^b have the meaning of the forward (backward) transfer and reflected amplitudes in the TLS-free region. After some algebra, we obtain $t_r^a = t_l^a \equiv t^a$, which guarantees the no discontinuity in the value of the wave function. With Eqs. (9-11), the transfer and reflected amplitudes read

$$t^a = \frac{-2g_a g_b \sin k}{v_g(E-\omega_A) + g_b^2 \sin(2k) + i\left(2g_b^2\sin^2 k + g_a^2\right)}, \tag{19}$$

$$r^b = -\frac{v_g\left(E-\omega_A+\frac{g_b^2}{\xi}e^{-ik}\right)+ig_a^2}{v_g\left(E-\omega_A+\frac{g_b^2}{\xi}e^{ik}\right)+ig_a^2}. \tag{20}$$

In this case, the probability for finding the photon in CRW-a (b) is equal to the transfer rate $T_b^a \equiv 2|t^a|^2$ (reflectance $R_b^b \equiv |r^b|^2$). It is easily to find that $T_b^a + R_b^b = 1$ which guarantees the probability conservation for the incident photon.

When $g_a = 0$, the transfer amplitudes vanish. According to the probability conservation, all the incident waves get perfectly reflected. However, the phase of the reflected amplitude could be nonzero. As $g_a = 0$, the system becomes a semi-infinite CRW with a TLS inside. The hard-wall boundary due to the CRW termination reflects all the incident waves. The absorption and emission of single photons by the TLS introduce the phase different from π to the reflected amplitude, which is originated from the radiative properties of the TLS. It is well-known that spontaneous emission of a TLS depends on the electromagnetic vacuum environment that the atom is subjected to. Here, the boundary modifies the radiation field and acts back onto the TLS. According to the method of images [32], the radiated photon is reflected by the virtual

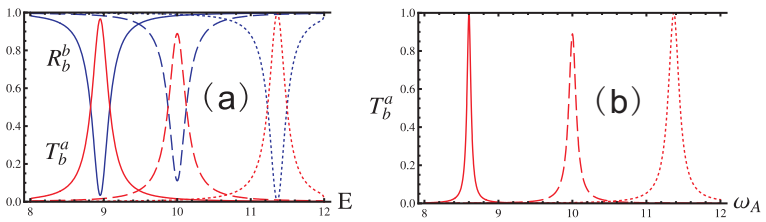

Fig. 3. The probabilities for finding single photons in the CRW-a (blue line) and the CRW-b (red line). (a) The probabilities as a function of the incident energy E. The parameters are the same in Fig. 2(a). (b) The coefficient $T_b^a(E)$ as a function of the atomic energy splitting ω_A, The parameters are the same in Fig.2(b).

$j_b = 0$ cavity. Consequently, the excited state of the TLS is dressed by its own radiation field with the Lamb shift $\Delta(E) = g_b^2 \cos k/\xi$ and the decay rate $\Gamma_b(E) = 2g_b^2 \sin^2 k/v_g$ of the TLS into the waveguide modes of the CRW-b, where the group velocity $v_g = 2\xi \sin k$. In the weak-coupling limit $g_b \to 0^+$, the transition frequency of the TLS is renormalized as $\omega_A + \Delta(\omega_A)$. Actually, the changes in the radiative rates of the TLS can be qualitatively understood by the following consideration. First, let us explain how the factor two appears in Γ_b. In an infinite CRW, the TLS radiates amplitude α to the upward, so does it to the downward. Therefore the total rate of the atomic energy loss into an infinite CRW is proportional to $2|\alpha|^2$. In the presence of a perfect mirror, light originally radiated to the downward is reflected back toward the TLS and interferes with the light originally radiated to the upward. For constructive interference, the total amplitude is 2α. And the total rate of the atomic energy loss into an semi-infinite CRW is proportional to $4|\alpha|^2$, which is twice larger than the total rate of the single atom embedded in the infinite CRW. Now, we concern the factor $\sin^2 k$ appearing in Γ_b. For a TLS inside an infinite CRW, g_b is the coupling strength between the continuum and the TLS. Then, we obtain $2|\alpha|^2 = g_b^2/v_g$. However, for the TLS inside a semi-infinite CRW, the coupling strength between the continuum and the TLS is modified as $g_b \sin k$ by the Fourier transformation. Consequently, we obtain $4|\alpha|^2 = \Gamma_b$.

With $g_a \neq 0$, the CRW-a provides an extra channel for the radiated photon. Transferring becomes possible after the incident photon is absorbed by the TLS. Therefore, the transfer rate should be related to both the coupling strength g_a and the modified coupling strength $g_b \sin k$ by the boundary, which is why T_b^a in Eq. (19) has the product of g_a and $g_b \sin k$ in its numerator. The coupling of the TLS to the extra channel introduces additional atomic energy loss, which is characterized by the decay rate Γ_a. Hence, the decay rate of the TLS is the sum of Γ_a and Γ_b, which construct the imaginary part of the denominator in Eqs. (14)-(15) and (19)-(20). Since the energy-level shift caused by the CRW-a is zero, the real part of the denominator in Eqs. (14)-(15) and (19)-(20) only contains the atomic transition energy ω_A and the Lamb shift $\Delta(E)$ introduced by the semi-infinite CRW. One can also observe that the transfer amplitudes in Eqs. (15) and (19) have the same expression. However, the transfer rate T_b^a is twice larger than T_a^b. According to studies in the previous section, the maximum T_b^a could be one. By comparison, we plot the probabilities for finding the photon in each CRW in Fig.3 with the parameters same to Fig. 2. Obviously, the reflectance R_b^b could be lower than 50%, even down to zero. Actually, it is not difficult to find that a peak of the transfer rate occurs when the incident energy satisfies the resonant condition $E - \omega_A + \Delta(E) = 0$ for the given coupling strengths. The results in [20, 21] told us that the decay rates should be equal to further improve the transfer rate, i.e., the incident energy should further satisfies $2g_b^2 \sin^2 k = g_a^2$ (called decay-match condition), which requires that $g_a \leq \sqrt{2} g_b$. The above discussion told us that when the coupling and hopping strengths are fixed, one can adjust ω_A to achieve the maximal value one of the transfer rate for the photon

with a given incident energy.

4. Conclusion

In this work, we have analytically studied the scattering process of single photons in a T-shaped waveguide with a TLS embedded in the node of the T junction, where the T-shaped waveguide is made of two CRWs —an infinite CRW (refer to CRW-*a*) and a semi-infinite CRW (refer to CRW-*b*). Comparing to the observations in [20, 21] with the X-shaped waveguide which made of two noninteracting infinite CRWs, the boundary introduces new physical features: 1) There are transmission and reflection in the incident CRW-*a*, but only reflection in the incident CRW-*b*. Consequently, the probabilities for finding the photon in CRW-*a* and CRW-*b* have different expressions, for example, $R_a^a + T_a^a$ in CRW-*a* and T_a^b in CRW-*b* for waves incident from the CRW-*a*, and T_b^a in CRW-*a* and R_b^b in CRW-*b* for waves incident from the CRW-*b*. 2) The probability for successfully transferring the photon is different. The maximum magnitude of the transfer rate is 50% for waves incident from the CRW-*a*, however, 100% for waves incident from the CRW-*b*. Since 50% is the maximum probability for transferring single photons from one CRW to the other in the previous schemes [20,21], the boundary indeed enhance the transfer probability. We note that since the linear response of the TLS is considered, the results could apply to the equivalent classical model of coupled oscillators.

Acknowledgments

This work is supported by NSFC No. 11374095, No. 11422540, No. 11434011, No. 11575058; NBRPC No. 2012CB922103; Hunan Provincial Natural Science Foundation of China (11JJ7001, 12JJ1002). Z. H. Wang is supported by Postdoctoral Science Foundation of China (under Grant No. 2014M560879).